Even after 1320 min, when about 75% of the units are oxidized, only 16% of the oxidized units are found in sequences with more than eight oxidized units. A similar conclusion can be drawn from Figure 6. It shows that up to $t_{exptl.} \simeq 630$ min the sequences with one reacted unit contribute more to $y(t)$ than any other type of sequences, and up to $t_{exptl} \simeq 1150$ min the sequences with two reacted units have the largest contribution to $y(t)$.

As previously shown by one of us,[11] the extent of reaction of periodate oxidated amylose is well described by the present model of nearest-neighbor cooperative effects. Hence, it will be very interesting to see whether experiments confirm the validity of the theory to describe sequences of reacted units. Dr. T. Painter will attempt to carry out an experiment to this effect.

Acknowledgment. This work was incited by a discussion remark from Professor B. U. Felderhof. Therefore we are especially indepted to him. One of us (J.J.G.) would like to thank the Institut of Festköperforschung der Kernforschungsanlage, Jülich, for hospitality, and Norges Tekniske Høgskoles Fond, Norway, for financial support.

References and Notes

(1) T. Painter and B. Larsen, *Acta Chem. Scand.*, **24**, 813 (1970).
(2) M. F. Ishak and T. Painter, *Acta Chem. Scand.*, **25**, 3875 (1971).
(3) J. B. Keller, *J. Chem. Phys.*, **37**, 2584 (1962); **38**, 325 (1963).
(4) T. Alfrey, Jr., and W. G. Lloyd, *J. Chem. Phys.*, **38**, 322 (1963); **39**, 1903 (1963).
(5) D. A. McQuarrie, J. P. McTague, and H. Reiss, *Biopolymers*, **3**, 657 (1965).
(6) A. Silberberg and R. Simha, *Biopolymers*, **6**, 479 (1968). See also P. Rabinowitz, A. Silberberg, R. Simha, and E. Loftus, *Adv. Chem. Phys.*, **15**, 281 (1969).
(7) E. A. Boucher, *J. Chem. Soc., Faraday Trans. 1*, **68**, 2295 (1972); *J. Chem. Soc., Faraday Trans. 2*, **69**, 1839 (1973).
(8) J. J. González, P. C. Hemmer, and J. S. Høye, *Chem. Phys.*, **3**, 228 (1974).
(9) J. J. González and P. C. Hemmer, *J. Polym. Sci., Polym. Lett. Ed.*, **14**, 645 (1976).
(10) J. J. González and P. C. Hemmer, *J. Chem. Phys.*, **67**, 2496 (1977); **67**, 2509 (1977).
(11) J. J. González, *Biophys. Chem.*, **2**, 23 (1974).
(12) J. J. González, Avhandling for den tekniske doktorgrad, Trondheim, 1977, and *Macromolecules*, in press.
(13) P. C. Hemmer and J. J. González, *J. Polym. Sci., Polym. Phys. Ed.*, **15**, 321, (1977).
(14) B. Widom, *J. Chem. Phys.*, **44**, 3888 (1966); **58**, 4043 (1973).
(15) B. U. Felderhof, *J. Stat. Phys.*, **6**, 21 (1972).
(16) T. H. Barron, R. J. Bawden, and E. A. Boucher, *J. Chem. Soc., Faraday Trans. 2*, **70**, 651 (1974).
(17) O. Smidsrød, B. Larsen, and T. Painter, *Acta Chem. Scand.*, **24**, 3201 (1970).
(18) T. Painter and B. Larsen, *Acta Chem. Scand.*, **24**, 2724 (1970).
(19) Barron, Bawden, and Boucher[16] have analyzed another model, the random pairwise occupation of a linear array. They were able to derive the distribution of reacted sequences as a function of time. Their model is, for an infinite lattice, equivalent to our special case with complete inhibition of neighbor units.

Studies on the Deformation Mechanism of Polyethylene Spherulites by the Orientation Distribution Function of Crystallites[1a]

Masaru Matsuo,*[1b] Kazumi Hirota,[1b] Kenichi Fujita,[1c] and Hiromichi Kawai[1c]

Department of Textile Engineering, Faculty of Engineering, Yamagata University, Yonezawa 992, Japan, and the Department of Polymer Chemistry, Faculty of Engineering, Kyoto University 606, Japan. *Received August 9, 1977*

ABSTRACT: A deformation mechanism of a polyethylene spherulite under uniaxial stretching is discussed on the basis of the crystallite orientation distribution function obtained by the distribution functions of a reciprocal lattice vector of 13 crystal planes. The distribution functions for each crystal plane at the extension ratio $\lambda = 1.4$ are observed in detail by X-ray diffraction. The result is actually demonstrated that the evaluation of the deformation mechanism already suggested by many authors is correct. That is, the crystallite orientation distribution function reflects the fact that the deformation mechanism is dependent upon the rotation of crystallites around their own *b* axes associated with the lamellar rotation in the equatorial region as well as around their own *a* axes associated with the rotation of crystallites within lamellae in the meridian region. Moreover, the orientation distribution function of the crystal *c* axes has a peak around polar angle $\theta_j = 30°$, which has never been observed directly because of the weak intensity of X-ray diffraction. On the other hand, the preferential orientation of crystal *c* axes is found to be dependent upon the distribution of a principal stress having the highest magnitude in the stretching direction. This relation suggests that since tie-chain molecules are strained, the crystal *c* axes orient gradually parallel to the stretching direction.

I. Introduction

There have been a number of papers[2-16] concerning the deformation mechanism of polymer spherulites. Quantitative investigations have been reported for polyethylene spherulites by Stein et al.,[3,4] Kawai et al.,[6,8,14,15] and Moore.[10] They compared the experimental results observed from X-ray diffraction technique with the theoretical ones calculated from the model considering the orientation of crystallites or/and that of crystal lamellae in addition to the affine deformation of the spherulite. The evaluation for their comparison is classified into two methods. One is in terms of the second-order orientation factors of orientation distribution functions of principal axes of the crystal unit cell $F_{20}{}^{j}$ ($j = a, b, c$).[3,4,6,8,10] The other is in terms of the orientation distribution functions of the reciprocal lattice vector of the crystal plane.[14-16] The former is only due to an apparent aspect of the orientation distribution, and one cannot discuss the crystal orientation in detail. However, it may suffice for the characterization of simple textures. Theoretical investigations of general arrangements of crystallites were mainly carried out by Wilchinsky[17,18] and Sack.[19] Their investigations have demonstrated that it is possible to deduce from other data the value of the second-order orientation factor of a plane whose diffraction is too weak to observe. The latter is a direct comparison between the experimental and theoretical distribution functions reflecting the deformation mechanism. Hence, the latter is superior to the former.

0024-9297/78/2211-1000$01.00/0

The investigation of the latter has been carried out by Nomura et al.[14,15] with respect to the principal axes of the crystal unit cell and the reciprocal lattice vector of (110) crystal plane which gives the most intense reflection in X-ray diffraction, assuming two steps in the deformation in accordance with recent studies[3,20–24] on rheo-optical behavior of polymer spherulite, that is: (1) instantaneous deformation of the spherulite, associated with orientation of lamellar axis and untwisting of crystal lamella; and (2) reorientation of crystallites within the oriented lamellae after a considerable time lag. The theoretical calculation on the basis of their assumption was carried out by means of a mathematical representation of the relationship among the orientation distribution functions of the crystal lamella within the spherulite, the crystal unit cell, and the reciprocal lattice vectors in terms of series expansions to the generalized spherical harmonics. The models[14,15] were tested experimentally with respect to the distributions of the (110) and (200) crystal planes, and the theoretical results were in fairly good agreement with the experimental ones.

This paper is concerned with the deformation mechanism of crystallites within the spherulite on the basis of the orientation distribution function of crystallites which is determined from the functions of the reciprocal lattice vector of 13 crystal planes observed from X-ray diffraction measurement. This method affords the best means of studing the deformation mechanism of crystallites, because one may pursue directly the deformation mechanism of polymer spherulites through the orientation distribution function of the crystallites.

The outstanding method of evaluation was first proposed as a general description of crystal orientation by Roe and Krigbaum[25–27] and applied to determine the orientation distribution of the (002) crystal plane as well as the orientation function of crystallites of a cross-linked polyethylene sample crystallized at fixed strain. The diffraction intensity for the (002) crystal plane observed with the previous X-ray instrument was so weak that the fiber axis orientation could not be measured. This method was applied to the fiber texture of polyethylene terephthalate[28] as well as the biaxial case for polyethylene.[29]

In this paper, the deformation mechanism of polyethylene spherulites will be discussed on the basis of the orientation distribution function of crystallites as well as that of crystal c axes by using the method of Roe and Krigbaum.[25–27] According to the above results, the model[15] which has been proposed on the basis of the comparison between the experimental and theoretical results for the orientation distribution function of reciprocal lattice vector of the (110) crystal plane will be reexamined. This reexamination is the main aim of this paper. Moreover, the preferential orientation of the crystal c axes to the stretching direction will be discussed in relation to the distribution of the principal stress within the spherulite.

II. Experimental Section

A. Test Specimen and Experimental Procedure. As discussed already, a high-density polyethylene, Sholex 5065, was used as the test specimen. The pellets of the high-density polyethylene were melted at 180 °C for 10 min in the laboratory press under a pressure of 200 kg/cm^2, slowly cooled to 80 °C, and annealed for an hour. The film obtained was quenched by being plunged into an ice water bath. The volume percent crystallinity which was measured by the ethanol–water density gradient tube method was found to be 76%. The film thickness is 300 μm. The specimen was uniaxially stretched at 60 °C to the extension ratio $\lambda = 1.4$. The stretching temperature was actually the lowest one at which the stretching was performed uniformly without any necking phenomena. The extension ratio $\lambda = 1.4$ is the highest

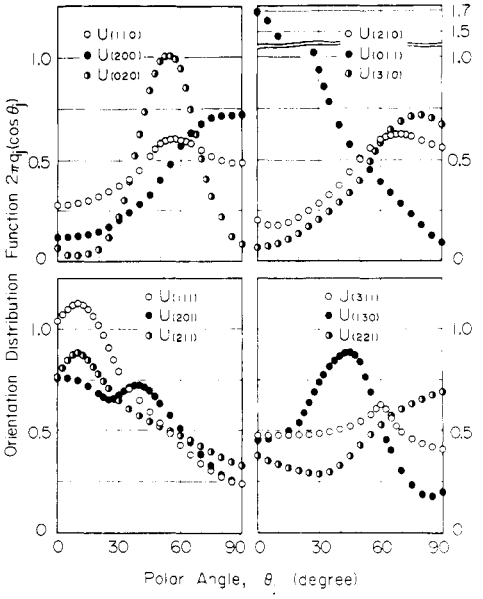

Figure 1. Orientation distribution functions for the reciprocal lattice vector of 12 crystal planes observed from X-ray diffraction.

one at 60 °C for the sample thickness 300 μm. In this measurement, the intensity of X-ray is set at 100 milliampere–40 kV and the width of the divergent, scattering, and receiving slits are 1/6°, 1/6°, and 0.15 mm, respectively. Before the X-ray measurement, we confirmed that the spherulite in this specimen was deformed from sphere to ellipsoid by means of small-angle light scattering.

The X-ray diffraction measurement was carried out for the equatorial direction with respect to the 13 crystal planes at a fixed value of θ_j denoting the polar angle between the stretching direction and the reciprocal lattice vector of the jth crystal plane. The change of polar angle θ_j was carried out at proper intervals from 0 to 90°. This process may be achieved by the rotation of the specimen around its thickness direction. The scanning speed with regard to Bragg angle $2\theta_B$ is one-eighth degree per minute. After applying correction to the observed X-ray diffraction intensity (for air scattering, background noise, polarization, and absorption) and substracting the contribution of the amorphous halo from the corrected total intensity curve, the equatorial diffraction curve may be obtained as the function of the Bragg angle $2\theta_B$. This intensity curve is believed to be due to the contribution of the diffraction intensity from the crystalline phase. The intensity curve $I_{crys}(2\theta_B)$ is separated into the contribution from the individual crystal planes on the assumption that each peak has a symmetric form given by a Lorenz function of $2\theta_B$ as shown in eq 1, where I_j^0 is the maximum intensity of the jth peak,

$$I_{crys}(2\theta_B) = \sum_j \frac{I_j^0}{1 + (2\theta_0^j - 2\theta_B)^2/(\beta_j/2)^2} \qquad (1)$$

β_j is the half-width of the jth peak, and θ_0^j is the Bragg angle at which the maximum intensity of the jth peak appears. As a result, there is quite good agreement between the observed and calculated results except for a slight disagreement.

B. Experimental Results and Discussion. Figures 1 and 2 show the orientation distribution functions $2\pi q_j(\cos\theta_j)$ of a reciprocal lattice vector of 13 crystal planes. As seen in Figure 1, the functions of the (110) and (200) crystal plane are relatively similar to the experimental results of Yukalon YK-300 extended at room temperature.[15] That is, the distributions of the (110) and (200) crystal planes have a peak around θ_j = 55 and 90°, respectively. On the other hand, the distribution function of the (002) crystal plane was observed directly from the X-ray diffraction technique. The distributin has a peak around polar angle θ_j = 30°. This mode is quite different from the fact presumed by many authors[3,4,6,8] on the basis of the orientation factor of crystal c axes calculated from the orientation factors of the (110) and (200) crystal planes by using Wilchinsky's equation. It is understood that the crystal c axes orient preferentially to the stretching

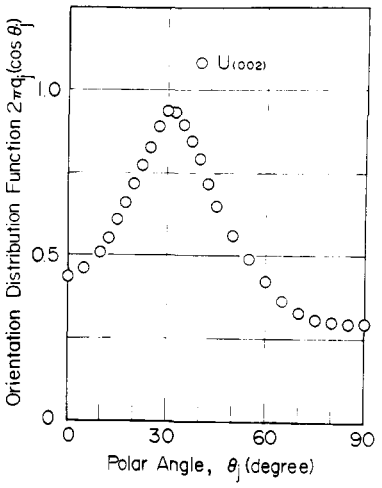

Figure 2. Orientation distribution function for the crystal c axes observed from X-ray diffraction.

Table I
Average Degree of Uniaxial Orientation of the Reciprocal Lattice Vector of the jth Crystal Plane

jth crystal plane	$\langle\cos^2\theta_j\rangle$	jth crystal plane	$\langle\cos^2\theta_j\rangle$
(110)	0.2971	(201)	0.4297
(200)	0.2087	(211)	0.4122
(210)	0.3222	(311)	0.3403
(020)	0.2535	(130)	0.4440
(011)	0.5449	(221)	0.2514
(310)	0.2070	(002)	0.4429
(111)	0.4766		

direction, i.e., the distribution function of the crystal c axes has a peak at polar angle $\theta_j = 0°$, though they have never been observed directly as an orientation distribution function because of the weak intensity of the X-ray diffraction. Hence, we tried to evaluate the accuracy of our experimental results. Table I reveals the average degree of uniaxial orientation of the reciprocal lattice vector of 13 crystal planes obtained by the results in Figures 1 and 2, in which the summation of three quantities for the (200), (020), and (002) crystal planes is almost unity. This result suggests that the experimental results for the (200), (020), and (002) crystal planes in Figures 1 and 2 are correct. Moreover, we investigated the accuracy of the experimental results for the other crystal planes. That is, the average degree of the crystal c axes was calculated by using Wilchinsky's equation[18] on the basis of the average of the reciprocal lattice vector of the (110) crystal plane which has the strongest intensity of X-ray diffraction. Table II reveals the results obtained, in which the calculated results are rather close to the experimental ones for the eight crystal planes. However, as for the crystal (011), (111), (211), (130), and (221) planes, the calculated results differ considerably, though the separation from superposed peak was carried out in detail by using eq 1. This result suggests $2\pi q_j(\cos\theta_j)$ of the jth crystal plane still contains the contribution with regard to the function of the other crystal planes. Hence we introduce the parameter C_{ji} as the relative normalized weight of reciprocal lattice vector to obtain the value of $2\pi q_j(\cos\theta_j)$ better. This method has been discussed in detail by Roe and Krigbaum.[25-27]

III. Discussion

Figure 3 shows the geometrical interrelations of two Cartesian coordinates $0\text{–}X_1X_2X_3$ and $0\text{–}U_1U_2U_3$ fixed within the bulk specimen and crystallites, respectively. The orientation of the structural unit within the space of the film specimen may be specified by using three Euler angles, ϕ, θ, and η, as shown in Figure 3a. The angles θ and ϕ, which define the orientation of U_3 axis of the unit within the space, are the polar and azimuthal angles, respectively, and η specifies the rotation of the unit around its own U_3 axis. The orientation of the jth axis with

Table II
Average Degree of Uniaxial Orientation of the Crystal c Axes[a]

jth crystal plane	$\langle\cos^2\theta_j\rangle$	jth crystal plane	$\langle\cos^2\theta_j\rangle$
(200)	0.4550	(201)	0.4687
(210)	0.4563	(211)	0.6599
(020)	0.4374	(311)	0.4173
(011)	0.5749	(130)	0.6779
(310)	0.4762	(221)	0.6422
(111)	0.5457		

[a] Calculated by using Wilchinsky's equation on the basis of the average degree of the reciprocal lattice vector of the (110) crystal plane and that of the jth crystal plane listed. Average degree of uniaxial orientation of the crystal c axes observed from the X-ray diffraction technique is 0.4429 as listed in Table I.

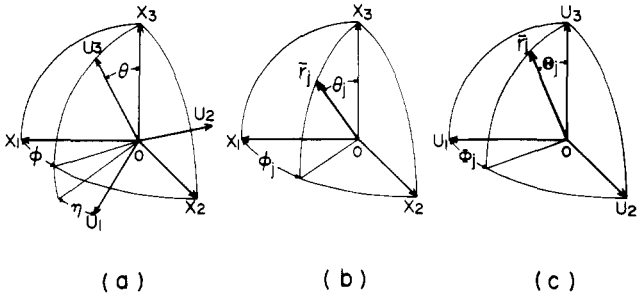

Figure 3. Cartesian coordinate illustrating the geometrical relation (a) Eulerian angles θ, η which specify the orientation of coordinate $0\text{–}U_1U_2U_3$ of structural unit with respect to coordinate $0\text{–}X_1X_2X_3$ of specimen. (b) Angles θ_j and ϕ_j which specify the orientation of the given jth axis of the structural unit with respect to the coordinate $0\text{–}X_1X_2X_3$. (c) Angles Θ_j and Φ_j which specify the orientation of the jth axis of the structural unit with respect to the coordinate $0\text{–}U_1U_2U_3$.

respect to the $0\text{–}X_1X_2X_3$ is given by the polar angle θ_j and the azimuthal angle ϕ_j as shown in Figure 3b. Moreover, the jth axis within the unit cell is specified by the polar angle Θ_j and the azimuthal angle Φ_j as shown in Figure 3c.

For uniaxial stretching, ϕ and ϕ_j as shown in Figure 3 are random. Hence, the orientation distribution function $\omega(\theta,\eta)$ of crystallites may be calculated from $q_j(\cos\theta_j)$ by using the method proposed by Roe et al.,[25-27] which is given by

$$F_{l0}^{\,j} = \langle P_l(\cos\theta_j)\rangle = \int_0^{2\pi}\int_0^{\pi} q_j(\cos\theta_j)P_l(\cos\theta_j)\sin\theta_j\,d\theta_j\,d\phi_j \quad (2)$$

$$F_{l0}^{\,j} = F_{l00}P_l(\cos\Theta_j) + 2\sum_{n=2}^{l}\frac{(l-n)!}{(l+n)!}F_{l0n}P_l^{\,n}(\cos\Theta_j)\cos n\Phi_j \quad (3)$$

$$4\pi^2\omega(\theta,\eta) = \sum_{l=0}^{\infty}\frac{(2l+1)}{2}F_{l00}P_l(\cos\theta) + 2\sum_{l=2n=2}^{\infty}\sum^{l}\frac{(2l+1)}{2}\frac{(l-n)!}{(l+n)!}F_{l0n}P_l^{\,n}(\cos\theta)\cos n\eta \quad (4)$$

where l and n are even integers. $P_l^{\,n}(x)$ and $P_l(x)$ are the associated Legendre's polynomial and Legendre's polynomial, respectively. In actual calculation, the lth order orientation factor $F_{l0}^{\,j}$ with regard to the jth crystal plane was calculated by eq 5 instead of eq 3. This is due to the insufficiency of the separation of superposed peaks by eq 1. Equation 5 may be given by

$$F_{l0}^{\,j} = F_{l00}\sum_i C_{ji}P_l(\cos\Theta_{ji}) + 2\sum_{n=2}^{l}\frac{(l-n)!}{(l+n)!}F_{l0n}\sum_i C_{ji}P_l(\cos\Theta_{ji})\cos n\Phi_{ji} \quad (5)$$

Table III
Parameters for the Plane-Normal Orientation Distribution Function $2\pi q_j(\cos\theta_j)$

no.	$2\theta_B$ (Bragg angle), deg	jth plane	superposed planes	C_{ji}
1	21.62	(110)		
2	24.02	(200)		
3	30.15	(210)		
4	74.42	(002)		
5	36.38	(020)		
6	39.79	(011)	(011)	0.713
			(310)	0.287
7	40.85	(310)	(310)	0.484
			(011)	0.264
			(111)	0.252
8	41.69	(111)	(111)	0.616
			(310)	0.167
			(201)	0.217
9	43.07	(201)	(201)	0.634
			(220)	0.234
			(111)	0.132
10	47.01	(211)		
11	55.00	(311)	(311)	0.774
			(130)	0.226
12	57.32	(130)	(130)	0.581
			(221)	0.419
13	57.61	(221)	(130)	0.406
			(221)	0.594

The derivation of eq 5 was discussed in detail by Roe and Krigbaum.[25,26] In this paper, the values of C_{ji} are obtained by using the simplex method. The simplex method is a sort of direct research method to obtain the object function on the basis of trial and error and is useful, particularly, to optimize the parameters contained in the function which is difficult to differentiate. C_{ji} is determined by the attempt which minimizes eq 6.

$$R_2 = \frac{\sum_l \{(F_{l0}^j)_{\text{orig}} - (F_{l0}^j)_{\text{cal}}\}^2}{\sum_l (F_{l0}^j)^2_{\text{orig}}} \qquad (6)$$

After a somewhat complicated calculation, the value of R_2 is 27% and consequently the value of C_{ji} may be obtained as listed in Table III. The value of R_2 is not superior to that obtained already for cross-linked polyethylene by Roe and Krigbaum.[25,26] However, the orientation functions $2\pi q_j(\cos\theta_j)$ calculated with the use of reconstructed F_{l0}^j values which are obtained without the contribution of the observed jth crystal reflection,[26] that is, the full curve, are in good agreement with the experimental data as shown in Figure 4. Moreover, $2\pi q_j(\cos\theta_j)$ calculated with the use of reconstructed F_{l0}^j values[26] is found to be nearly equal to the full curve in Figure 4. Hence, we do not show these values as a figure.

By using the reconstructed F_{l0}^j values, the orientation distribution function $\omega(\theta,\eta)$ of the crystallites may be calculated. The infinite series for l is terminated at l = 24. The number order of crystal planes used to obtain the coefficients F_{l0n} in accord with that of the jth crystal plane are listed in Table III.

Figure 5 shows the contour map representing the orientation function $4\pi^2\omega(\theta,\eta)$. The shaded areas having the negative density which arises due to the inaccuracy of the reconstructed F_{l0}^j value as well as the series termination error are found to be very small in this calculation. The orientation distribution function $\omega(\theta,\eta)$ has the two peaks around θ = 27°, η = 24° and θ = 38°, η = 75°, respectively. This result seems to indicate that the former mainly depends on the rotation of crystallites around their own b axes associated with the lamellar rotation in the equatorial region, while the latter depends on the rotation of crystallites around their own a axes associated with the rotation of crystallites within the lamellae in the meridian region.

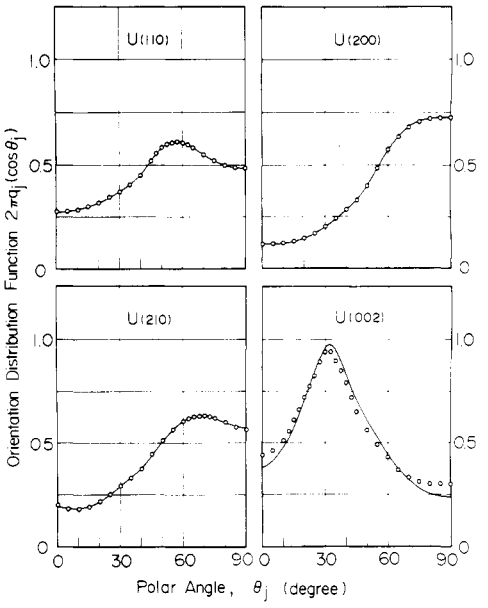

Figure 4. Orientation distribution functions of reciprocal lattice vector about four reflections calculated with the use of reconstructed F_{l0}^j values which were obtained without the contribution of the observed jth crystal plane, (a) the observed (110) reflection, (b) the observed (200) reflection, (c) the observed (210) plane, and (d) the observed (002) plane.

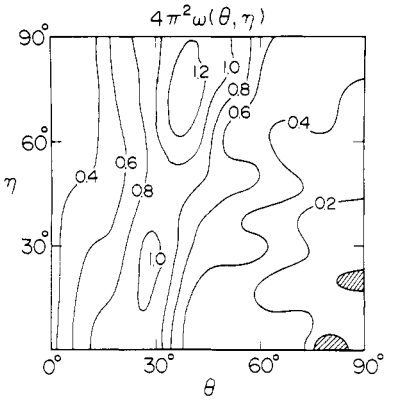

Figure 5. Orientation distribution function of the crystallites derived from the orientation distribution functions for the 13 crystal planes observed from X-ray diffraction.

The two types of the orientation seem to be due to the behavior of tie-chain molecules which connect the mosaic structures within adjacent crystal lamellae to each other. Actually, this explanation may be derived from the average degree of uniaxial orientation of the noncrystalline chain segments assumed to correspond to the tie-chain molecules. The degree of orientation is found to be $\langle\cos^2\theta_a\rangle$ = 0.5018 by using a similar procedure to that proposed by Stein et al.[32] (or Takahara et al.[33]) based on the simple additivity of crystalline and noncrystalline contributions to the total (bulk) birefringence of the specimen. Comparing the average degree of orientation of noncrystalline chain segments with that of crystal c axes, the degree of preferential orientation to the stretching direction of noncrystalline chain segments is superior to that of the crystal c axes. Hence, the tie-chain molecules are strained and the crystal c axes gradually orient parallel to the stretching direction. In the equatorial region, the orientation of crystal c axes is mainly due to the rotation around their

Table IV
Direction of Coordinate Axes

coordinate system	direction of X_i, V_i, and U_i axes	
	$i = 1$	$i = 3$
$0\text{-}X_1X_2X_3$	normal to film surface	stretching direction of film specimen
$0\text{-}V_1V_2V_3$	normal to lamellar surface containing OV_2 and OV_3 axes	lamellar axis grown radially within a spherulite
$0\text{-}U_1U_2U_3$	crystal a axis of polyethylene crystallite	crystal c axis of polyethylene crystallite

Table V
Euler Angles of Coordinate Transformations

ref coordinate	Euler angles	oriented coordinates
$0\text{-}X_1X_2X_3$	ϕ',θ',η'	$0\text{-}V_1V_2V_3$
$0\text{-}X_1X_2X_3$	ϕ,θ,η	$0\text{-}U_1U_2U_3$
$0\text{-}V_1V_2V_3$	α,β,γ	$0\text{-}U_1U_2U_3$

b axes, while in the meridian region, around their a axes.

Next, we investigate whether the orientation distribution function $\omega(\theta,\eta)$ calculated from the model for the deformation mechanism of polyethylene spherulites is in agreement with $\omega(\theta,\eta)$ shown in Figure 5. Although the model is essentially the same as that proposed for low-density polyethylene,[15] slight changes of the model are made.

Tables IV and V show the geometrical interrelations of three Cartesian systems, $0\text{-}X_1X_2X_3$, $0\text{-}V_1V_2V_3$, and $0\text{-}U_1U_2U_3$ fixed within the bulk specimen, crystal lamella, and crystallites, respectively. The directions of the coordinate axes of each Cartesian system are given in Table IV and the Euler angles of coordinate transformations among the three Cartesian systems are given in Table V.

The first step of the spherulite deformation, the instantaneous orientation of crystal lamellae including untwisting, can be represented by the orientation of the Cartesian system $0\text{-}V_1V_2V_3$, with respect to the Cartesian system $0\text{-}X_1X_2X_3$ and can be formulated for uniaxial deformation as follows:

$$\omega'(\theta',\eta') = \frac{W_0}{8\pi^2}\{1 + \sigma(\lambda - 1)(1 - \cos^2\theta') \times \cos^{2J_A}\eta'\}\lambda^3/\{\lambda^3 - (\lambda_3 - 1)\cos^2\theta'\}^{3/2} \quad (7)$$

where $\omega'(\theta',\eta')$ is an orientation distribution function of the crystal lamellae with respect to the Cartesian system $0\text{-}X_1X_2X_3$, σ and J_A are parameters characterizing the ease and sharpness of instantaneous lamellar untwisting, respectively, and W_0 is a normalization constant.

The second step of the spherulite deformation, the delayed reorientation of crystallites within the lamella, can be represented by the orientation of the Cartesian coordinates $0\text{-}U_1U_2U_3$ with respect to the Cartesian coordinates $0\text{-}V_1V_2V_3$. The corresponding distribution function may be formulated as follows:

$$q(\beta,\alpha,\gamma) = \frac{Q_0}{8\pi^2}\{f_r - f_c(\lambda - 1)[R(\theta')/R_0]^{J_C}P(\theta') + [(1 - \cos^2\beta)\cos^2\alpha\sin^2\gamma]^{J_B} + f_c(\lambda - 1)[R(\theta')/R_0]^{J_C}(\sin^4\theta' - \cos^4\beta + 2\cos^2\theta'\cos^2\beta)(f_{er} + \cos^{2l_c}\alpha)(f_{ar} + \sin^{2m_c}\gamma)\} \quad (8)$$

In the undeformed state ($\lambda = 1$), eq 8 reduces to

$$q(\beta,\alpha,\gamma) = \frac{Q_0}{8\pi^2}\{f_r + [(1 - \cos^2\beta)\cos^2\alpha\sin^2\gamma]^{J_B}\} \quad (9)$$

Q_0 is a normalization constant. On the right side of eq 9, the first term ($Q_0f_r/8\pi^2$) corresponds to the fraction of crystallites within the lamella that have random orientation; in the undeformed state, it is a measure of the degree of imperfection of the lamella in the undeformed state. The second term, $\{Q_0[(1 - \cos^2\beta)\cos^2\alpha\sin^2\gamma]^{J_B}/8\pi^2\}$, corresponds to the fraction of crystallites with the b axis oriented parallel to the lamellar axis; this term has a maximum value when the b and c axes of the crystal are perfectly oriented in the directions of the lamellar axis (V_3, grown direction) and lamellar normal (V_1, thickness direction), respectively, as listed in Table IV. In eq 8 and 9, J_B is a parameter characterizing the sharpness of the distribution function; i.e., J_B is zero or infinite, which means the orientation is random or perfect, respectively.

In order to represent the crystal c axes orientation parallel to the stretching direction due to straining of the tie-chain molecules in the deformed state, the term ($\sin^4\theta' - \cos^4\beta + 2\cos^2\theta'\cos^2\beta$) in eq 8 is introduced in such a manner that the term has a maximum value when the angle β becomes identical to θ' of the lamellar orientation. Two types of c axis orientation are postulated on the basis of (a) the c axis orientation associated with simple rotation of the crystallite around its own a axis and (b) the c axis orientation associated with random rotation of the crystallite around its own c axis. They differ in their effects as indicated by the insertion of the final term in eq 9; i.e., the orientation of type (a) is mostly affected by the factor $\cos^{2l_c}\alpha$ and $\sin^{2m_c}\gamma$, while the orientation of type (b) is affected by the factors f_{er} and f_{ar} in eq 8. In other words, when the factors f_{er} and f_{ar} are zero and the parameters l_c and m_c are infinite, the type (a) orientation is indicated, but, when the values of f_{er} and f_{ar} increase, the type (b) orientation predominates. The parameters l_c and m_c characterize the sharpness of the orientation distribution of the crystallites with respect to the angles α and γ, respectively.

The term $f_c(\lambda - 1)[R(\theta')/R_0]^{J_C}$ in eq 8 represents the fractional dependence of the c axis orientations of both types (a) and (b) on the extension ratio of the spherulite λ and of the lamella $R(\theta')/R_0$ in terms of the parameters f_c and J_C, where $R(\theta')$ is given by

$$R(\theta') = R_0\lambda\{\lambda^3 - (\lambda^3 - 1)\cos^2\theta'\}^{-1/2} \quad (10)$$

On the other hand, the term $f_c(\lambda - 1)[R(\theta')/R_0]^{J_C}P(\theta')$ in eq 8 is added in order to cancel out the variation of the constant Q_0 with the polar angle θ',[15,16] where $P(\theta')$ is given by

$$P(\theta') = \frac{1}{8\pi^2}\int_0^{2\pi}\int_0^{2\pi}\int_{-1}^{1}(\sin^4\theta' - \cos^4\beta + 2\cos^2\theta' \times \cos^2\beta)(f_{er} + \cos^{2l_c}\alpha)(f_{ar} + \sin^{2m_c}\gamma)\,d(\cos\beta)\,d\alpha\,d\gamma \quad (11)$$

The term $f_c(\lambda - 1)[R(\theta')/R_0]^{J_C}P(\theta')$ corresponds to the fraction of crystallites within the lamella that have random orientation such as the term f_r.[15]

A test of the proposed model of spherulitic deformation was performed by comparing the calculated orientation distribution function $2\pi q_j(\cos\theta_j)$ for a specified crystal plane, that is, the (110) crystal plane, with $2\pi q_j(\cos\theta_j)$ observed from the X-ray diffraction experiment at extension ratio $\lambda = 1.4$ of the test specimen. Although the number of parameters in eq 7 and 8 seems to be too large to deduce an explicit conclusion, the values of the parameters giving the best fit of calculated and observed results may also be determined easily by using the simplex method.[30,31] Actually, the parameters in eq 7 and 8 were determined by the attempt which was made to minimize

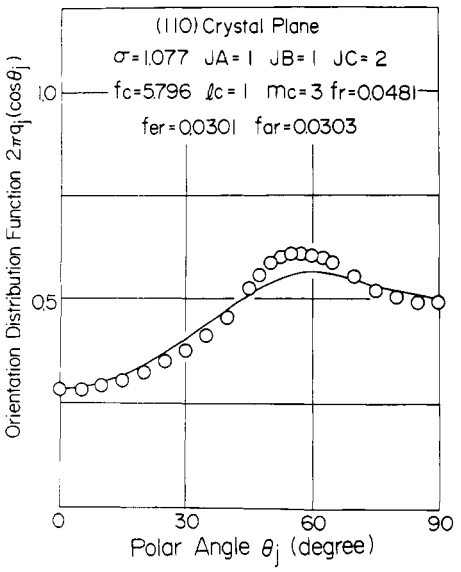

Figure 6. Comparison of orientation distribution function for the reciprocal lattice vector of the (110) crystal plane observed from X-ray diffraction, with that calculated from eq 7 and 8. The parameters are selected to minimize the average square error between the calculated and experimental results.

the average square error given by the following equation. That is:

$$\text{av sq error} = \frac{\left\{\int_0^{2\pi}\int_0^{\pi} W(\theta_j)[q_j(\cos\theta_j)_{\text{exp}} - q_j(\cos\theta_j)_{\text{cal}}]\sin\theta_j\, d\theta_j\, d\phi_j\right\}^2}{\left\{\int_0^{2\pi}\int_0^{\pi} q_j(\cos\theta_j)_{\text{exp}}\sin\theta_j\, d\theta_j\, d\phi_j\right\}^2} \quad (12)$$

where, the jth crystal plane is the (110) crystal plane and $W(\theta_j)$ is the weight varied with the polar angle θ_j.

Figure 6 shows the comparison between the experimental and the calculated results, in which the average square error is 2.63% on the assumption that $W(\theta_j)$ is unity at any polar angle. This value is the smallest one as far as eq 7 and 8 are employed as the deformation model of a polyethylene spherulite. The peak of the calculated (110) distribution is broader than that of the experimental distribution. The reason is due to the selection of the weight. In this calculation, the weight was not selected on the basis of fitting the peak position of the calculated (110) distribution with that of the experimental one, but selected on the basis of minimizing the average square error when $W(\theta_j)$ is unity independent to the polar angle θ_j, as discussed above. Among the values of the parameters f_{er}, f_{ar}, l_c, and m_c shown in Figure 6, the values of f_{er} and f_{ar} are much smaller than unity. This fact suggests that the mode of crystal c axes orientation is not dependent upon the random rotation of the crystallites around their own c axes, but upon the rotation of the crystallites around their own a axes.

Figure 7 shows the orientation distribution function of the crystal a, b, and c axes calculated on the basis of the same parameter listed in Figure 6. The calculated result of the crystal a axis is rather close to the experimental one shown in Figure 3. As for the crystal b axis, the calculated and experimental distributions are similar. That is, the former has a peak around $\theta_j = 45°$, while the latter is around $\theta_j = 55°$. However, the peak of the experimental distribution is much sharper and higher than that of the calculated one. On the other hand, for the crystal c axis, the shapes of both distributions are quite different. The

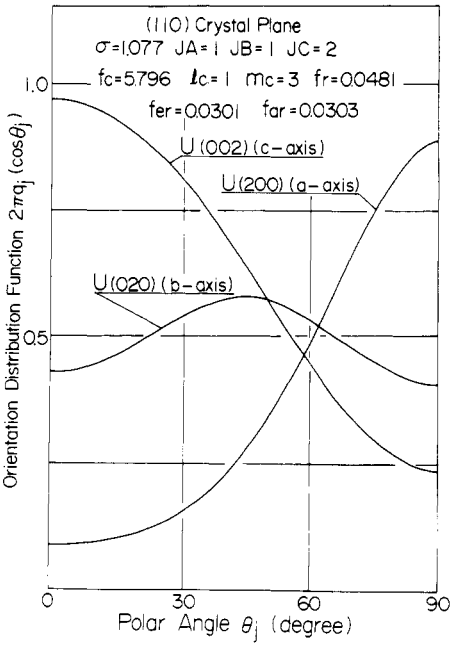

Figure 7. Orientation distribution functions of the crystal a, b, and c axes calculated by using the same parameters listed in Figure 6.

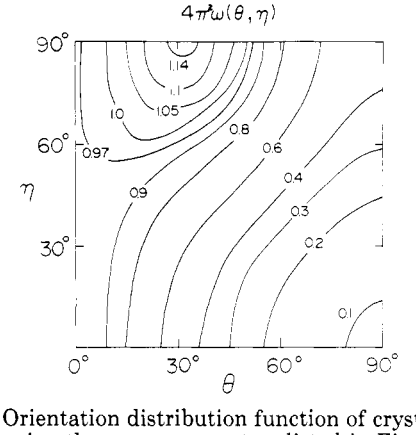

Figure 8. Orientation distribution function of crystallites calculated by using the same parameters listed in Figure 6.

calculated distribution has the peak at $\theta_j = 0°$, which suggests the preferential orientation of the crystal c axis to the stretching direction. The reason resides in the term $(\sin^4\theta' - \cos^4\beta + 2\cos^2\theta'\cos^2\beta)$ in eq 8; this term has a maximum value when the crystal c axis within lamella orients parallel to the stretching direction at any extension ratio. This term was introduced on the basis of the second-order orientation factor of crystal c axes reported by many authors,[3,4,6,8,10] as discussed already. The theoretical distribution $2\pi q_j(\cos\theta_j)$ calculated from eq 7 and 8 is in fairly good agreement with the experimental one for the (110) and (200) crystal planes. However, the calculated distribution for the crystal c axes is different from the experimental one shown in Figure 2. That is, as discussed already, the distribution has a peak around polar angle $\theta_j = 30°$. This model will have to be modified with respect to the term $(\sin^4\theta' - \cos^4\beta + 2\cos^2\theta'\cos^2\beta)$ in eq 8 to be in fairly good agreement with the experimental result in the case of extension ratio $\lambda = 1.4$, which, however, seems to be a very difficult problem.

Figure 8 shows the contour map representing the orientation distribution function $\omega(\theta,\eta)$ of crystallites. This map has a peak around $\theta = 30°$, $\eta = 90°$. However, the map has no peak at the rather lower angle of η, as appeared in the map of Figure 5 calculated from the X-ray dif-

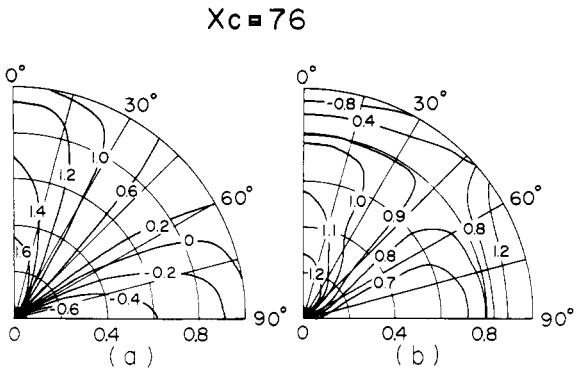

Figure 9. Distribution of principal stresses (a) P_1 and (b) P_2 within the spherulite calculated by using a linear isothermal static elastic theory for the value of crystallinity 76%, in which scale numbers, 0, 0.4, and 0.8, mean the degree of (r/a), while values of scale listed in circumference mean the degree of polar angle. a is the radius of the spherulite.

fraction data. This result suggests that this model reflects the rotation of crystallites around their own a axes, but is hardly affected by the untwisting of crystal lamellae, illustrating the rotation of crystallites around their own b axes. In other words, the model which is performed on the basis of the fit of the calculated and observed results for $2\pi q_j(\cos\theta_j)$ about a particular crystal plane such as (110) plane does not reveal the detailed mechanism with regard to the orientation of crystallites within the spherulite under uniaxial stretching.

Recently, the orientation distribution function $2\pi q_j(\cos\theta_j)$ was obtained by Yoon and Stein[34] on the basis of a similar model[35] used in the calculation of light scattering from deformed three-dimensional spherulites. The theoretical result is in rather good agreement with the experimental one with respect to the crystal (110) and (200) planes. This method seems to be somewhat complicated for the calculation of the crystallite orientation function $\omega(\theta,\eta)$.

Finally, we investigate the relationship between the crystal orientation at extension ratio $\lambda = 1.4$ and the distribution of the principal stresses within the spherulite. However, the method is basically incorrect, because the former belongs to the category of a large deformation, while the latter belongs to that of a small deformation. Hence, in this paper, the comparison was carried out to investigate the relationship approximately. The three different principal stresses may be given by

$$P_1 = \sigma_{rr}\cos^2\Delta\theta + 2\sigma_{r\theta}\sin\Delta\theta\cos\Delta\theta + \sigma_{\theta\theta}\sin^2\Delta\theta$$

$$P_2 = \sigma_{rr}\sin^2\Delta\theta - 2\sigma_{r\theta}\sin\Delta\theta\cos\Delta\theta + \sigma_{\theta\theta}\cos^2\Delta\theta \quad (13)$$

$$P_3 = \sigma_{\phi\phi}$$

where

$$\tan 2\Delta\theta = 2\sigma_{r\theta}/(\sigma_{rr} - \sigma_{\theta\theta}) \quad (14)$$

In actual calculation, four kinds of stresses σ_{ij} were obtained on the basis of a linear isothermal elastic theory.[36-38] The five elastic stiffnesses used in this calculation were obtained by the same method used in a previous paper.[38]

Figure 9a,b shows the calculated distribution function of the principal stresses P_1 and P_2, respectively, in which the magnitude of P_1 is larger than that of P_2 as a whole. The distribution of P_1 shows the higher magnitude in the stretching direction $\theta = 0°$. Moreover, as a point on the radial direction at $\theta = 0°$ moves to the center of the spherulite, the magnitude at the point increases. Considering Figure 9 again, the distribution of P_1 integrated to the radial part is postulated to have a maximum magnitude at polar angle $\theta = 0°$. This result suggests that in the direction of the meridian, the tie-chain molecules are strained strongly, and consequently the crystal c axes with orientation perpendicular to the lamellar axis in the undeformed state orient gradually parallel to the stretching direction by rotation of the crystallites around their own a axes with increase of the extension ratio.

IV. Conclusion

The crystal orientation $\omega(\theta,\eta)$ within a polyethylene spherulite under uniaxial stretching was obtained by the orientation function of a reciprocal lattice vector of 13 crystal planes. The distribution of the crystal c axes has a peak around polar angle $\theta_j = 30°$ at extension ratio $\lambda = 1.4$. This result is different from the preferential orientation of the crystal c axes to the stretching direction postulated by many authors on the basis of the second-order orientation factor of the crystal c axes calculated from the orientation factor of the (110) and (200) crystal planes by using Wilchinsky's equation. Moreover, the model which is essentially the same as one proposed for a low-density polyethylene was tested by experiment for the (110) crystal plane. The theoretical distribution was in fairly good agreement with the experimental one. However, the theoretical distribution for the crystal c axes as well as the crystallites was found to be insufficient to explain the experimental one. That is, the theoretical distribution of the crystal c axes has a peak at $\theta_j = 0°$, while that of crystallites only has a peak around $\theta = 30°$, $\eta = 0°$. This fact suggests that it is a dubious procedure to evaluate the deformation mechanism of a polymer spherulite on the basis of the fit of the calculated and observed results for the orientation distribution function of a reciprocal lattice vector of a particular crystal plane such as the (110) crystal plane. Finally, the orientation of the crystal c axes was found to be related to the distribution of the principal stress P_1 within the spherulite. This result suggests that the tie-chain molecules are strained, and consequently the crystal c axes orient gradually parallel to the stretching direction.

Acknowledgment. The authors are indebted to Associate Professor Shunji Nomura, Faculty of Textile Science, Kyoto University of Industrial Arts and Textile Fibers, for his valuable suggestions. Thanks are also due to Mr. Shoji Suehiro, Faculty of Engineering, Kyoto University, for his valuable discussion in constructing the program of the simplex method.

References and Notes

(1) (a) Presented partly at the 26th Annual Meeting of the Society of Polymer Science, Japan, Kyoto, May 1977; (b) Yamagata University; (c) Kyoto University.
(2) Z. W. Wilchinsky, *Polymer*, **5**, 271 (1964).
(3) K. Sasaguri, S. Hoshino, and R. S. Stein, *J. Appl. Phys.*, **35**, 47 (1964).
(4) K. Sasaguri, R. Yamada, and R. S. Stein, *J. Appl. Phys.*, **35**, 3188 (1964).
(5) I. L. Hag and A. Keller, *Kolloid-Z.*, **204**, 43 (1965).
(6) T. Oda, S. Nomura, and H. Kawai, *J. Polym. Sci., Part A*, **3**, 1993 (1965).
(7) K. Kobayashi and T. Nagasawa, *J. Polym. Sci., Part C*, **No. 15**, 163 (1966).
(8) T. Oda, N. Sakaguchi, and H. Kawai, *J. Polym. Sci., Part C*, **No. 15**, 223 (1966).
(9) R. S. Samuels, *J. Polym. Sci., Part C*, **No. 20**, 253 (1967); *J. Polym. Sci., Part A-2*, **6**, 1101 (1968).
(10) R. S. Moore, *J. Polym. Sci., Part A-2*, **5**, 711 (1967).
(11) R. G. Crystal and D. Hausen, *J. Polym. Sci., Part A-2*, **6**, 981 (1968).
(12) T. Oda, N. Sakaguchi, and H. Kawai, *Kobunshi Kagaku*, **25**, 588 (1968).
(13) T. Oda, M. Motegi, M. Moritani, and H. Kawai, *Kobunshi Kagaku*, **25**, 639 (1968).

(14) S. Nomura, A. Asanuma, S. Suehiro, and H. Kawai, *J. Polym. Sci., Part A-2*, **9**, 1991 (1971).
(15) S. Nomura, M. Matsuo, and H. Kawai, *J. Polym. Sci., Polym. Phys. Ed.*, **10**, 2489 (1972).
(16) M. Matsuo, H. Hattori, S. Nomura, and H. Kawai, *J. Polym. Sci., Polym. Phys. Ed.*, **14**, 223 (1976).
(17) Z. W. Wilchinsky, *J. Appl. Phys.*, **30**, 792 (1959).
(18) Z. W. Wilchinsky, *J. Appl. Phys.*, **31**, 1969 (1960).
(19) R. A. Sack, *J. Polym. Sci.*, **54**, 543 (1961).
(20) P. Erhardt and R. S. Stein, *J. Polym. Sci., Part B*, **3**, 553 (1965).
(21) R. S. Stein, T. Tanaka, E. Chang, and I. Kimura, ONR Technical Report No. 111, Polymer Research Institute, University of Massachusetts, Amherst, Mass., August 1968.
(22) T. Hashimoto, O. J. Phillips, and R. S. Stein, paper presented at the IUPAC Meeting, Leiden, The Netherlands, September 1970.
(23) T. Oda and R. S. Stein, *J. Polym. Sci., Part A-2*, **10**, 685 (1972).
(24) T. Hashimoto, H. Kawai, and R. S. Stein, paper presented at the 19th Symposium on Rheorogy, Japan, Nagoya, October 1971.
(25) R. J. Roe and W. R. Krigbaum, *J. Chem. Phys.*, **40**, 2608 (1964).
(26) W. R. Krigbaum and R. J. Roe, *J. Chem. Phys.*, **41**, 737 (1964).
(27) R. J. Roe, *J. Appl. Phys.*, **36**, 2024 (1965).
(28) W. R. Krigbaum and Y. I. Balta, *J. Phys. Chem.*, **71**, 1770 (1967).
(29) W. R. Krigbaum, T. Adachi, and J. V. Dawkins, *J. Chem. Phys.*, **49**, 1532 (1968).
(30) W. Spendly, G. R. Hext, and F. R. Himsworth, *Technometrics*, **4**, 441 (1962).
(31) J. A. Nelder and R. Mead, *Comput. J.*, **7**, 308 (1965).
(32) R. S. Stein and F. H. Norris, *J. Polym. Sci.*, **21**, 381 (1956).
(33) H. Takahara, S. Nomura, H. Kawai, Y. Yamaguchi, K. Okazaki, and A. Fukushima, *J. Polym. Sci., Part A-2*, **6**, 197 (1968).
(34) D. Y. Yoon, C. Chang, and R. S. Stein, *J. Polym. Sci., Polym. Phys. Ed.*, **12**, 2091 (1974).
(35) J. J. van Aartsen and R. S. Stein, *J. Polym. Sci., Part A-2*, **9**, 295 (1971).
(36) T. T. Wang, *J. Appl. Phys.*, **44**, 4052 (1973).
(37) T. T. Wang, *J. Polym. Sci., Polym. Phys.* Ed., **12**, 445 (1974).
(38) M. Matsuo, T. Ogita, S. Suehiro, T. Yamada, and H. Kawai *Macromolecules*, **11**, 521 (1978).

Effects of Casting Solvents on Mechanical and Structural Properties of Polydiene-Hydrogenated Polystyrene–Polyisoprene–Polystyrene and Polystyrene–Polybutadiene–Polystyrene Block Copolymers

R. Séguéla and J. Prud'homme*

Department of Chemistry, University of Montreal, Montreal Quebec, Canada H3C 3VI. *Received May 1, 1978*

ABSTRACT: Stress–strain and dynamic mechanical measurements were carried out over a range of temperatures for a polyisoprene-hydrogenated SIS block copolymer and for a polybutadiene-hydrogenated SBS block copolymer having polystyrene endblocks of about the same molecular weights close to 1×10^4 and having styrene weight fractions of 0.22 and 0.29, respectively. Specimens were prepared by solvent casting from solutions in heptane, cyclohexane, and toluene. Microdomain structures were investigated by small-angle X-ray scattering. Depending upon the casting solvent, the hydrogenated SIS copolymer exhibited spherical or cylindrical polystyrene structures while the hydrogenated SBS copolymer exhibited spherical, cylindrical, or lamellar polystyrene structures. The three structures were obtained in the order of increasing solvent affinity for polystyrene. The mechanical behavior of the specimens with spherical microdomains was very close to those of unfilled vulcanized rubbers. In contrast, specimens with cylindrical structures showed stress softening on repeated extensions and those with lamellar structures showed yield and neck propagation in the first extension. The systematic change of microdomain structure with increasing solvent affinity for polystyrene is interpreted in terms of solvent partition within the micellar arrangement produced during the casting process. Also discussed are the relations between domain sizes and unperturbed chain dimensions for the three types of structures observed.

In a previous paper[1] we reported physical and mechanical properties of a polyisoprene-hydrogenated polystyrene–polyisoprene–polystyrene (SIS) elastomeric block copolymer containing 22% by weight of styrene. The copolymer showed two glass transitions at −67 and ~90 °C, respectively, and its stress–strain curves measured at room temperature in successive extension cycles ($0 < \epsilon \leq 3$) were nearly reversible and superposable, indicating a microphase system in which the polystyrene cross-linking domains were discrete and particularly well isolated. In contrast, the original SIS copolymer showed irreversible stress softening in the first extension cycle. Both specimens were prepared by solution casting at room temperature using cyclohexane as solvent. Cyclohexane is a poor solvent for polystyrene and a good solvent for both polyisoprene and hydrogenated polyisoprene. As will be shown in the present paper, we also have observed that a polybutadiene-hydrogenated SBS block copolymer containing 29% by weight of styrene does not exhibit the stress-softening effect when cast from heptane, a non-solvent for polystyrene but a good solvent for hydrogenated polybutadiene.

Solution casting from preferential solvents for polydienes is known[2-5] to improve the rubber-like behavior of SIS and SBS block copolymers having a styrene content in the range of 15 to 30% by weight. Such solvents swell preferentially the polydiene phase and thereby give rise to a better dispersion of the polystyrene phase which after complete solidification of the material appears as discrete glassy domains in a continuous rubbery matrix. However, it has been observed[2,6] that SIS and SBS films cast from preferential solvent for the polydienes exhibit stress softening on repeated extensions. This phenomenon was attributed to irreversible processes such as rupture of interconnections between some of the glassy domains or deformation of the latter. It is similar to the Mullins effect in reinforced rubbers. The stress-softening phenomenon also occurs for compression molded or extruded specimens[2,7-9] but, as shown by Pedemonte et al.,[9] it disappears when such specimens are swollen with a

0024-9297/78/2211-1007$01.00/0